Multifunctional $a_v\beta_6$ Integrin-Specific Peptide–Pt(IV) Conjugates for Cancer Cell Targeting

Anne C. Conibear[†,∥,iD], **Sonja Hager**[‡,∥], **Josef Mayr**[§], **Matthias H. M. Klose**[§], **Bernhard K. Keppler**[§], **Christian R. Kowol**[§,iD], **Petra Heffeter**[*,‡], and **Christian F. W. Becker**[*,†,iD]

[†]Faculty of Chemistry, Institute of Biological Chemistry, University of Vienna, Währinger Straße 38, 1090 Vienna, Austria

[‡]Institute of Cancer Research and Comprehensive Cancer Centre, Medical University of Vienna, Borschkegasse 8a, 1090 Vienna, Austria

[§]Institute of Inorganic Chemistry, University of Vienna, Faculty of Chemistry, Währinger Straße 42, 1090 Vienna, Austria

Abstract

Increasing the specificity of cancer therapy, and thereby decreasing damage to normal cells, requires targeting to cancer-cell specific features. The $a_v\beta_6$ integrin is a receptor involved in cell adhesion and is frequently up-regulated in cancer cells compared to normal cells. We have selected a peptide ligand reported to bind specifically to the β_6 integrin and have synthesized a suite of multispecific molecules to explore the potential for targeting of cancer cells. A combination of solid-phase peptide synthesis and chemoselective ligations was used to synthesize multifunctional molecules composed of integrin-targeting peptides, cytotoxic platinum(IV) prodrugs, and fluorescent or affinity probes joined with flexible linkers. The modular synthesis approach facilitates the construction of peptide–drug conjugates with various valencies and properties in a convergent manner. The binding and specificity of the multifunctional peptide conjugates were investigated using a cell line transfected with the β_6 integrin and fluorescence microscopy. This versatile and highly controlled approach to synthesizing labeled peptide–drug conjugates has the potential to target potent cytotoxic drugs specifically to cancer cells, reducing the doses required for effective treatment.

[iD]**ORCID**
Anne C. Conibear: 0000-0002-5482-6225
Christian R. Kowol: 0000-0002-8311-1632
Christian F. W. Becker: 0000-0002-8890-7082

[*]**Corresponding Authors:** christian.becker@univie.ac.at. Phone: + 43-1-4277-70510. Fax: + 43-1-4277-9705; petra.heffeter@meduniwien.ac.at. Phone: +43-1-40160-57594. Fax: + 43-1-40160-957557.
[∥]**Author Contributions**
A.C.C. and S.H. contributed equally to the manuscript.

Notes
The authors declare no competing financial interest.

Introduction

Antibody–drug conjugates have shown promising results in cancer therapy because they couple the cytotoxic activity of small molecule drugs with the specificity of antibodies for cancer cell markers, thereby reducing the amount of damage to other cells.[1–3] Peptides are also increasingly being used for selective cancer targeting in peptide–drug conjugates because they can bind with high specificity to receptors over-expressed on tumor cells.[4,5] Whereas the attachment of drug molecules to antibodies is mostly restricted to conjugation at free lysine amines or to cysteine thiols, peptides offer a wider variety of conjugation options because of their synthetic accessibility. The former strategy of conjugation to free lysine or cysteine residues, although successfully employed for the synthesis of the two antibody–drug conjugates on the market (brentuximab vedotine and trastuzumab emtansine), can yield heterogeneous products with a distribution in the antibody-to-drug ratio and provides only very limited control over the regioselectivity of drug attachment.[1,3] In contrast, conjugation of a drug to a synthetic peptide can be precisely controlled. In addition to the targeting role of peptides, the properties of cell-penetrating peptides and the properties of self-assembling peptides to form nanostructures of various kinds have also been used for drug delivery.[5,6]

Selective conjugation of a drug to a peptide or antibody via chemoselective ligation strategies allows the generation of conjugates with defined targeting moiety-to-drug ratios and precise localization of the drug.[7,8] Approaches involving enzymatic conjugation, engineered cysteine residues or glycan modification have shown potential; however, biorthogonal conjugation enables an even-greater degree of control over the drug conjugation.[3,8,9] Introduction of biorthogonal functionalities into recombinantly expressed proteins can be achieved with enzymatic modification (often in combination with genetically introduced tags) or amber codon suppression but remains challenging.[10] In contrast, the chemical synthesis of peptides or protein fragments allows the flexible and site-specific incorporation of biorthogonal functionalities (for example, azides and alkynes for copper-catalyzed azide–alkyne click (CuAAC) ligation, maleimides for thiol–maleimide ligation, and ketones or aldehydes and aminooxy groups for oxime ligation).[8,11] Furthermore, peptides can be readily optimized and modified to study and improve the targeting properties to cancer cells and to develop cleavable linkers for the conjugation of cytotoxic drugs.[12,13]

Taking advantage of the flexibility and versatility afforded by peptide synthesis, we designed a series of peptide–drug conjugates to target a platinum(IV) prodrug specifically to cancer cells. The branched Y-shaped scaffold (**Y**) is composed of a short peptide linker, a biotin tag, and two monodisperse polyethylene glycol (PEG_{27}) polymers (Figure 1) that provide spatial separation between the two targeting peptides. Alkyne functionalities on the termini of the PEG_{27} chains allow the chemoselective ligation to integrin-targeting peptides (**P1**) via CuAAC ligation[14,15] and a cysteine residue on the scaffold allows for thiol–maleimide ligation[16] to either an oxaliplatin-based platinum(IV) prodrug (**oxali-Pt**)[17] or a fluorescent label (**Cy5**). The monodisperse PEG_{27} polymers were selected for their flexibility, hydrophilicity, and chemical inertness. In addition, the length of the PEG_{27} chain mimics the approximate distance between the Fc and Fab portions of an antibody[18] and might allow the simultaneous binding of the two targeting peptides to their receptors, increasing the affinity.

The peptide–platinum(IV) drug conjugate, however, differs significantly from an antibody–drug conjugate in that it is much smaller (~7 kDa compared to ~150 kDa for an antibody–drug conjugate) and is generated entirely by chemical synthesis. The peptide–drug conjugate (**oxali-Pt–Y1**) is designed for a modular assembly so that any of the functionalities can be exchanged easily for optimization or screening.

We selected the RGD-containing decapeptide **P1** that binds to the $a_v\beta_6$ integrin to target the cytotoxic platinum(IV) prodrug to cancer cells.[19] Integrins are heterodimeric transmembrane receptors that are involved in cell–cell and cell–substratum adhesion and have an important role in cell proliferation and migration.[20] The β_6 integrin subunit dimerizes only with the a_v subunit, is specific to epithelial cells, and is up-regulated in cancer and wound healing but is not expressed in healthy adult tissue, making it a suitable cancer-specific target.[20] Oyama et al. identified a 20-mer RGD-containing peptide (TP H2009.1) from a phage-display screen and found it to be 300-fold more selective for lung cancer cells than normal cells.[21] Subsequent studies identified the binding target to be the $a_v\beta_6$ integrin, as supported by binding of TP H2009.1 phage to SW480 cells transfected with the β_6 integrin but not to untransfected cells.[22] In contrast to the cyclic RGD peptide c(RGDfK) and derivatives that target $a_v\beta_3$ and $a_v\beta_5$ integrins,[23,24] few examples of $a_v\beta_6$–targeting peptide–drug conjugates have been reported. Tetramers of TP H2009.1 were synthesized on a trilysine core, and the construct was found to localize to the nuclei and to block phage uptake more efficiently than the monomer, suggesting possible benefits of multimerization.[21,25] The 20-mer TP H2009.1 has also been conjugated to doxorubicin, to quantum dots, and to a PET label.[22,25–27] Further studies identified the first 10 residues (**P1**) with a C-terminal amide as the minimum binding domain, and an Alexa-488-labeled 10-mer was specific for $a_v\beta_6$-expressing cells and the mediated internalization of the β_6 integrin.[26] These studies suggested that **P1** is a suitable peptide for the selective targeting and uptake of the cytotoxic platinum(IV) complex to cancer cells.

The potent cytotoxic activity of DNA-coordinating platinum complexes has revolutionized cancer therapy and prompted several approaches to increase their specificity and thereby minimize the severe side effects that are often associated with their usage.[28,29] One such approach is to administer octahedral platinum(IV) prodrugs, which are reduced to the active square-planar platinum(II) complexes in the hypoxic and reductive environment of cancer cells.[29] In addition to being more inert than their platinum(II) counterparts and, thus, less likely to undergo undesired premature interactions with biomolecules before they interact with DNA, the platinum(IV) complexes provide the possibility of conjugating molecules at the axial positions that can be used for selective targeting of the complex.[29,30] For example, mono- or bismaleimide-bearing linkers at the axial position(s) of cis- and oxaliplatin-based platinum(IV) compounds have been used to conjugate the platinum(IV) complexes to thiol-containing proteins such as albumin.[16,17] This conjugation resulted in greatly increased plasma half-life and tumor accumulation in a mouse model compared to the respective succinimides, which are not able to bind to thiols. Furthermore, distinctly improved antitumor activity of the albumin-conjugated platinum(IV) derivative compared to the approved platinum(II) reference compound oxaliplatin was observed.[17] We therefore selected the monomaleimide functionalized cis- and oxaliplatin-based platinum(IV)

complexes (**cis-Pt** and **oxali-Pt**, Figure 1) for conjugation to the scaffold bearing the integrin-targeting peptide (**P1**) to enhance the selective targeting of platinum(IV) prodrugs to tumor cells.

Here, we describe the design and synthesis of the peptide-drug conjugate **oxali-Pt–Y-1** composed of a cytotoxic platinum(IV) prodrug (**oxali-Pt**) conjugated via a thiol–maleimide ligation to a core peptide–PEG$_{27}$ scaffold (**Y**) to which two β_6 integrin-targeting peptides (**P1**) are conjugated by CuAAC ligation (Figure 1). We explore the activity of **oxali-Pt–Y-1** in terms of its binding, uptake, and cytotoxicity on cells positive and negative for β_6 integrin. Furthermore, we demonstrate the versatility of the modular design by synthesizing related peptide conjugates bearing a cisplatin-based platinum(IV) prodrug (**cis-Pt–Y-1**), scrambled targeting peptides and a fluorescent label, which were used as control compounds or for visualization.

Results

Solid-Phase Peptide Synthesis of the Scaffold (Y) and Binder Peptides (P1)

The biotinylated scaffold for conjugation of the platinum(IV) prodrug and the targeting peptides was successfully synthesized by manual solid-phase peptide synthesis (SPPS) using the fluorenylmethoxycarbonyl (Fmoc)-protection strategy. The peptide Boc–C(StBu)–G–A–S–G–G–K(Mtt)–K(Mtt) was assembled on a biotin-linked resin. Next, the methyltrityl (Mtt) lysine side-chain protecting groups were removed leaving the N-terminal Boc group and cysteine-*t*-butylthio (StBu) group intact. Fmoc–NH–PEG$_{27}$–COOH was coupled to both of the lysine side chains, and the propargylglycine residues were coupled to the amino termini of both PEG$_{27}$ chains to provide the alkyne moieties for the CuAAC reaction. The peptide–PEG$_{27}$ construct (**Y**, structure in the Supporting Information) was cleaved from the resin (retaining the cysteine-*t*-butylthio protecting group) and purified by reverse-phase high-performance liquid chromatography (RP-HPLC). The scaffold for conjugation to the fluorescent label (structure in the Supporting Information) was synthesized similarly but differed in the core sequence to which the PEG$_{27}$ chains and propargylglycine residues were coupled. Manual SPPS was also used to synthesize the integrin-targeting **P1** peptides bearing an ε-azido lysine residue at the C-terminus (structure in the Supporting Information), separated from the targeting peptide sequence by a PEG$_3$ spacer. The peptides were characterized by electrospray ionization mass spectrometry (ESI-MS) and purified by RP-HPLC.

CuAAC Ligations of the Targeting Peptide (P1) to the Scaffold (Y)

The integrin-targeting peptides **P1** were ligated to the peptide–PEG$_{27}$ scaffold (**Y**) by a CuAAC reaction in a dimethylformamide (DMF)/water (4:1) mixture (Figure 2a). Double ligation of **P1** to both PEG$_{27}$ chains was complete within 15 min, and the product **Y-1** was purified by RP-HPLC (see the Supporting Information). The use of sodium ascorbate to reduce the copper(II) to copper(I) resulted in partial removal of the *t*-butylthio protecting group from the cysteine, but the two products could both be recovered and used in further reactions. Ascorbate was also found to modify the arginine residues in the integrin-targeting peptide, a phenomenon that we recently studied in more detail.[31] This modification of

arginine by ascorbate, which resulted in a side-product having a mass of +174 Da, could be minimized by decreasing the amount of ascorbate used and by quenching the reaction as soon as the CuAAC reaction was complete.[31] Scrambled versions of the integrin-targeting peptide (**scP1**) were also successfully prepared by SPPS and linked to the scaffold to yield **Y-sc1**, which was used as a nonbinding control. A monovalent construct in which only one PEG_{27} chain was coupled to the scaffold was also ligated to **P1** using a CuAAC ligation to give **Y-mono-1**.

Maleimide Ligation of Platinum(IV) Prodrugs (cis- and oxali-Pt) and Fluorescent Label (Cy5) to Y-1

Removal of the *t*-butylthio protecting group from the cysteine of **Y-1** with tris(2-carboxyethyl)phosphine (TCEP) afforded the free thiol after isolation by RP-HPLC. The maleimide-functionalized platinum(IV) prodrugs (**cis-** and **oxali-Pt**) were synthesized as previously described,[17] and the maleimide ligation was achieved by dissolution in freshly degassed water and addition to the thiol-bearing scaffold **Y-1** under argon (Figure 2a). The reaction reached completion in 20 min, and the peptide–drug conjugate **oxali-Pt–Y-1** could be recovered in good yield (88% after HPLC) and purity (Figure 2b). A trace amount of the ascorbate adduct was detected with MW 7673.5 (+ 174), which can be seen as a minor charge series in the mass spectrum in Figure 2b. Ligation of **cis-Pt** and Cy5–maleimides was carried out in a similar fashion, giving rise to **cis-Pt–Y-1** and a fluorescently labeled scaffold with two integrin-binding peptides **Cy5–Y-1** (see the Supporting Information). The platinum(IV) prodrug is stable in PBS (Figure S1) but is designed to be released on reduction to Pt(II), leaving the peptide scaffold to be disposed of.

Synthesis of Scaffold with Integrin-Binding Peptides (Y–1) by SPPS

To facilitate the synthesis of sufficient quantities of the peptide–drug conjugate **oxali-Pt–Y-1** for cellular uptake and ICP-MS experiments, we developed a second synthesis strategy. Although the modular synthesis route described above was successful, the need for HPLC purification of the individual peptides and the products after the CuAAC reaction and StBu removal led to a loss of material. In a faster route to generate the multimilligram quantities of peptide–drug conjugate required for ICP-MS studies, the residues of the integrin-binding peptides were assembled on resin rather than conjugated by CuAAC. The lysine residues on the scaffold **Y** were protected with 1-(4,4-dimethyl-2,6-dioxocyclohex-1-ylidine)-3-methylbutyl (ivDde), and the N-terminal residue was Boc–Cys with an *S*-trityl protecting group. After the removal of the ivDde protecting groups and coupling of the PEG_{27} chains, the two integrin-binding peptides **P1** were assembled simultaneously on both PEG_{27} chains. Cleavage from the resin afforded a peptide construct **Y-1** (structure in the Supporting Information) with a free thiol ready for maleimide ligation of the maleimide-bearing platinum(IV) compounds. The ligations of **cis-** and **oxali-Pt** were successfully carried out on the crude peptide and the peptide–drug conjugates **oxali-Pt–Y-1** (Figure 2c) and **cis-Pt–Y-1** (see the Supporting Information) were isolated by RP-HPLC. Although the platinum(IV) complex, scaffold, and targeting peptides are identical in the **oxali-Pt–Y-1** conjugates generated by both strategies, it should be noted that the chemical structures (and, hence, MW) differ in the linkage between the PEG_{27} chains and the C-terminus of the targeting

peptides; in the modular synthesis, the linkage is composed of the triazole formed during the CuAAC reaction between the propargyl glycine on the scaffold and the ε-azido lysine-PEG$_3$ spacer of the targeting peptide, and in the combined synthesis, the targeting peptide is linked directly to the PEG$_{27}$ chain by an amide bond (structures in the Supporting Information).

Transfection of Integrin β_6 into SW480 Cells

Transfection of the integrin β_6-negative cancer cell line SW480 with ITGB6, the gene encoding integrin β_6, allowed us to develop a system to test the integrin β_6 binding of the peptide–drug conjugates. Integrin β_6 (ITGB6)-negative SW480 cells32 were transfected with ITGB6 and subsequently enriched for their ITGB6 overexpression by fluorescence-activated cell sorting (FACS). Over-expression of integrin β_6 in the transfected cell lines, called SW480 ITGB6 low (before sorting) and SW480 ITGB6 high (after sorting), was confirmed by immunofluorescence using a commercially available integrin β_6 antibody conjugated to allophycocyanin (APC). As shown in Figure 3a, the allophycocyanin fluorescence approximately doubled on transfection of SW480 with ITGB6 (SW480 ITGB6 low) and increased 4-fold after sorting of the cells for their ITGB6 expression (SW480 ITGB6 high). Expression of integrin β_6 and its dimerization partner integrin α_v was also confirmed by Western blot (Figure 3b). Although both integrin β_6 and integrin α_v were detected in the transfected SW480 ITGB high cell line, the levels were low in comparison to the epidermoid carcinoma cell line A431, which endogenously expresses integrin β_6 (Figures 3b and S2).33 Nevertheless, binding studies were pursued with the SW480 cell line to compare the binding of the peptide–drug conjugates with an ITGB6-positive and an ITGB6-negative cell line.

Integrin β_6 Binding of Biotinylated Y-1 Conjugates

Binding experiments to the integrin β_6-transfected cell line SW480 ITGB6 high were carried out with the biotin-labeled construct **Y-1** without the platinum(IV) complex. This allowed the determination of the integrin β_6-dependent binding without any confounding cytotoxic effects of the prodrug. Initial experiments with scaffolds bearing one (**Y-mono-1**) and two (**Y-1**) copies of the integrin-targeting peptide **P1** indicated that the monovalent construct **Y-mono-1** does not show high binding (Figures 3d and S6) and so subsequent experiments focused on the bivalent construct **Y-1**. Figure 3c shows that titration of **Y-1** on integrin β_6-over-expressing SW480 ITGB6 high cells in relation to non-expressing SW480 cells resulted in a continuous increase in fluorescence intensity up to a concentration of 0.5 nM, demonstrating specific integrin β_6 binding with an approximate half-maximal binding concentration of 0.3 ± 0.1 nM (based on a one-site specific binding curve fit). In contrast, the nontargeting scrambled construct **Y-sc1** shows no fluorescence increase in integrin β_6-overexpressing SW480 ITGB6 high cells compared to non-expressing SW480 cells. Although **Y-1** binding appears to reach a maximum at 0.5 nM on SW480 ITGB6 high cells, binding continued to increase up to the highest concentration tested (2.5 nM) on A431 cells, corresponding to their higher integrin β_6 expression (Figures S2 and S3).

Integrin β_6 binding was also supported by fluorescence microscopy using biotin-labeled **Y-1** and **Cy5–Y-1**. SW480 and SW480 ITGB6 high cells were treated with biotin-labeled **Y-1**, **Y-mono-1**, or **Y-sc1** and then with avidin–FITC, and the relative fluorescence was quantified

(Figures 3d and S4–S6). The fluorescence of SW480 ITGB6 high cells treated with **Y-1** was significantly higher than those treated with **Y-sc1** or **Y-mono-1** and was also significantly higher than the integrin β_6-negative SW480 parental line. The Cy5-labeled construct **Cy5–Y-1** allowed the direct visualization of cellular uptake and intracellular localization in living cells. As shown in Figure 3e–f, after 10 min of treatment with 0.5 μM **Cy5–Y-1**, SW480 ITGB6 high cells displayed a higher fluorescence signal than the integrin β_6-negative SW480. Furthermore, in these experiments on living cells, the **Cy5–Y-1** appeared to be intracellular rather than bound to the cell membrane and tended to localize around the nucleus, possibly indicating a rapid internalization of **Y-1**. Nuclear localization has also been reported for the tetrameric **P1** peptide.[21]

Uptake and Cytotoxicity of oxali-Pt–Y-1 Peptide–Drug Conjugates

To confirm that the platinum(IV) complex is internalized along with the targeting **Y-1** construct, integrin β_6-dependent cell uptake of **oxali-Pt–Y-1** and the respective succinimide-functionalized platinum(IV) reference compound (**oxali-Pt–succ**; structure shown in the Supporting Information)[17] were quantified by ICP-MS. Figure 4a shows the results of incubating SW480 and SW480 ITGB6 high cells with 50 μM **oxali-Pt–Y-1** or **oxali-Pt–succ** for 3 h. This high concentration of the peptide–drug conjugate and platinum(IV) complex was necessary to reach the minimum detection range of the ICP-MS instrument and to compensate for the small amount recovered from the cell lysate. In agreement with the data on the APC-labeled conjugates, SW480 ITGB6 high cells had a significantly higher cell-associated platinum content than the parental SW480. Moreover, uptake of the platinum(IV) complex lacking the integrin β_6-targeting moieties showed no integrin β_6-selective increase. This demonstrates a selective uptake of **oxali-Pt–Y-1** by integrin β_6-over-expressing cells.

To investigate whether the novel peptide–drug conjugates had integrin β_6-selective anticancer activity, cell viability experiments were initially performed for 72 h, but no reduction in cell viability was observed (data not shown). This was thought to be due to insufficient reduction of platinum(IV) to the active platinum(II) compound within this time frame. Although previous studies suggest that oxaliplatin-based platinum(IV) compounds are reduced slower than cisplatin-based platinum(IV) compounds,[17] the rate, location, and mechanism of reduction in cells, and especially in tumors, is still poorly understood.[34,35] Cell viability experiments with **oxali-Pt–Y-1** were then carried out over 14 days, and the peptide–drug conjugate showed distinct integrin β_6-dependent activity in contrast to the respective unbound platinum(II) and platinum(IV) complexes (Figure 4b). Thus, in integrin β_6-negative cells, only a ~25% reduction in final cell count was observed, which was increased to 77% and 97% in SW480 ITGB6 low and high cells, respectively. In contrast, **Y-1** peptides without platinum loading had no anticancer activity on either SW480 or SW480 ITGB6 high cells under these conditions (Figure S7). Interestingly, ITGB6 transfection did not impact on the sensitivity to the clinically evaluated RGD-targeted cyclic peptide cilengitide (Figure S7), indicating that transfection with integrin β_6 alone is not sufficient to provide sensitivity to RGD binding. In A431 cells, which endogenously express integrin β_6, cytotoxicity became more apparent with increasing incubation times with **oxali-Pt–Y-1** and reached comparable levels to the unselective platinum(IV) succinimide **oxali-Pt–succ** after 14 days (Figure S8).

Discussion

The modular chemical synthesis and ligation strategy designed for **oxali-Pt–Y-1** demonstrates the flexibility with which biorthogonal functionalities for ligation can be introduced site-selectively, and the versatility with which the modules can be exchanged. For example, substitution of the β_6 integrin-binding peptides for peptides targeting other integrins or other receptors over-expressed on cancer cells could be easily achieved, leading to rapid optimization or tuning of affinity and specificity. Ligation of the cytotoxic drug could also be extended to other drugs in addition to the cis- and oxaliplatin-based prodrugs demonstrated in this study. The selection of two conjugation strategies in the modular design enables variation at two locations in the molecule, and several other combinations of ligations could be envisaged. However, the orthogonality of the two ligations needs to be considered carefully; for the **oxali-Pt–Y-1** peptide–drug conjugate, the CuAAC reaction of the targeting peptides was carried out before the maleimide reaction as the platinum(IV) prodrug might be unstable to the reducing agents in the CuAAC reaction mixture.

Once the modular design of **oxali-Pt–Y-1** had been established for the conjugation of **Y** to **P1** by CuAAC ligation and then to **oxali-Pt** by maleimide ligation, SPPS synthesis of **Y-1** followed by maleimide ligation of **oxali-Pt** to the crude peptide gave access to larger amounts of **oxali-Pt–Y-1** for biological assays. The chemoselective ligations in the modular strategy were efficient, and each of the ligation reactions was high-yielding. Nevertheless, a significant loss of material resulted from the need to purify the individual scaffold and binder peptides and the products of the CuAAC reaction and StBu removal by HPLC. Synthesizing the targeting peptides directly on the scaffold also avoids use of the CuAAC reaction with the associated ascorbate–arginine side-product. Nevertheless, the modular strategy offers greater versatility for screening, optimization, and small-scale binding assays. Both approaches, however, yield homogeneous products with a defined ratio of cytotoxic drug molecules to targeting peptides.

The Y-shaped modular design and two targeting peptides on the PEG_{27} linkers of the peptide–drug conjugates described here distinguish them from antibody–drug conjugates, small molecule–drug conjugates, and peptide–drug conjugates that have been described recently.[36,37] Multivalency of the **P1** β_6 integrin-targeting peptides has been shown to be advantageous;[21,25] however, further studies are necessary to determine the avidity effects of the targeting peptides and whether they are able to bind simultaneously to two different receptors. Tetramers of **P1** displayed on a lysine core were found to obstruct phage uptake more effectively than trimers, dimers, or monomers, but it is unlikely that the shorter PEG_{10} linkers used would allow simultaneous binding to two receptors.[26] Internalization of the integrin receptors on binding to the target peptides might also preclude simultaneous binding. Our results, however, show a higher internalization of the divalent construct **Y-1** than of the monovalent construct **Y-mono-1**.

Although the peptide–drug conjugates were designed for selective delivery of cytotoxic drugs to cancer cells, the conjugation of the fluorescent label Cy5 illustrates a further application of the versatile scaffold for imaging. Such fluorescently labeled peptide conjugates could be used to visualize receptor expression levels by fluorescence microscopy,

and other labels could be conjugated for applications such as PET imaging. For example, in a similar study, a c(RGDfK) peptide was conjugated to a platinum(IV) prodrug and a fluorescent label to image drug-induced apoptosis.[38]

Establishment of a stably transfected SW480 cell line expressing integrin β_6 enabled testing of the binding and specificity of **oxali-Pt–Y-1** and **Y-1** constructs and provided insights into the integrin β_6 dependency of binding and cytotoxicity. Although the transfection with integrin β_6 was successful, the relative expression levels were low in comparison to the A431 cell line, which endogenously expresses integrin β_6 at high levels. Furthermore, the dimerization partner integrin α_v was also minimally expressed in the SW480 cell line. Resulting reduced availability of the dimer integrin $\alpha_v\beta_6$ might therefore explain the moderate binding levels observed and rapid saturation of the binding sites at low concentrations. Nevertheless, the saturation of the binding sites at low concentrations indicates a high affinity of the peptide–drug conjugate for the integrin β_6-expressing cells. The half-maximal binding concentration of 0.3 ± 0.1 nM calculated from the binding experiments on SW480 ITGB6 high cells is in a similarly low nanomolar range to previously reported binding experiments.[26,27] These experiments, however, were conducted mostly with H2009 cells, and binding was determined by inhibition of phage uptake by tetrameric peptides, so the EC_{50} values cannot be directly compared. The selective and rapid uptake of the **Y-1** constructs demonstrated by fluorescence microscopy provides an additional explanation for modest binding to the surface of the transfected cells. Although it might make detection of the **Y-1** binding more difficult, rapid internalization is a desired property of the peptide–drug conjugates and should result in accumulation of the cytotoxic drug inside the cells, as supported by the ICP-MS results and selective cytotoxicity.

Integrin-targeting peptides have been used in several studies to target platinum(IV) prodrugs and other metal-based anticancer complexes to cancer cells; however, the majority of these studies used the well-known cyclic c(RGDfK) peptide that targets $\alpha_v\beta_3$ and $\alpha_v\beta_5$ integrins. [19] For example, a cisplatin-based platinum(IV) prodrug conjugated to either one or two RGD peptides (either linear or cyclic) showed higher cytotoxicity than nontargeted or nonconjugated controls.[39] Similar to our results, the RGD peptides themselves did not inhibit cell growth. Although this was not observed in our case, a dual cytotoxic effect of both the RGD peptide and the platinum drug could be beneficial from a therapeutic perspective and this property could be optimized by attaching other targeting peptides. In another study, c(RGDfK) peptides were conjugated to a picoplatin-based platinum(IV) prodrug in mono- and tetravalent form. Although both constructs increased the cytotoxicity of picoplatin, the tetravalent conjugate showed higher internalization, and cells expressing higher levels of integrin had higher intracellular platinum levels in ICP-MS studies, similar to our results.[40] A number of other recent studies have demonstrated the versatility of integrin-targeting RGD peptides in various constructs: conjugation to light-activated platinum(IV) and ruthenium(II) complexes,[41,42] conjugation to cisplatin prodrug-loaded carbon nanotubes,[43] and conjugation to platinum(IV) prodrug-encapsulated polymer nanoparticles.[44] In contrast to the above studies, in which the targeting peptide is conjugated directly to the platinum(IV) prodrug or to a nanomaterial, we have conjugated the $\alpha_v\beta_6$ integrin-targeting peptides to PEG_{27} chains that provide flexibility, solubility, and the

potential for simultaneous binding to two receptors. Furthermore, the bivalent construction described here is homogeneous, has a multifunctional scaffold that can also be used for imaging and targets a different integrin ($\alpha_v\beta_6$) to that targeted by c(RGDfK).

In conclusion, chemical synthesis and chemoselective ligation reactions were used to construct a multifunctional peptide–drug conjugate, **oxali-Pt–Y-1**, composed of two identical cancer targeting peptides, a cytotoxic platinum(IV) prodrug and a biotin or fluorescent tag. In initial biological assays, the **oxali-Pt–Y-1** construct showed integrin β_6-dependent selectivity for integrin-expressing cells, and the platinum(IV) complex was taken up selectively into cells and retained its cytotoxic activity. More extensive biological testing would provide further insights into the integrin receptor expression and internalization and the rate at which the platinum(IV) is reduced to platinum(II). This peptide–drug conjugate design has the potential to be expanded and adapted to combine alternative cancer-targeting peptides, cytotoxic drugs, and labels to increase the specificity of cancer therapy and imaging. Furthermore, higher drug loadings or alternative positions of the cytotoxic drug could be achieved to optimize selective targeting and cytotoxic properties.

Methods

Solid-Phase Peptide Synthesis

Peptides were synthesized by manual solid-phase peptide synthesis using the Fmoc protecting group strategy. Unless specified otherwise, amino acids (2.5 equiv) with standard side-chain protecting groups [Arg(Pbf), Asp(tBu), Gln(Trt), Ser(tBu), and Thr(tBu)] were used and coupled with 2-(1H-benzotriazol-1-yl)-1,1,3,3-tetramethyluronium hexafluorophosphate (HBTU, 2.4 eq., 0.5 M in DMF) and diisopropylethylamine (DIPEA, 5 equiv) for 30 min and then deprotected with piperidine (20% v/v in DMF, 3×5 min). Peptides were cleaved from the resin with trifluoroacetic acid (TFA)/triisopropylsilane (TIPS)/dimethylsulfide/H_2O (90:2.5:5:2.5, v/v/v/v) for 3 h followed by precipitation with cold diethyl ether and centrifugation. Crude peptides were dissolved in water/acetonitrile (ACN, 50:50 with 0.1% TFA) and lyophilized. Purification was carried out by RP-HPLC on a C4 column (Kromasil, 1%/min gradient of ACN 5–45% at 20 mL/min on a Waters AutoPurification HPLC/MS system). Peptide purity was monitored by electrospray ionization mass spectrometry (Waters 3100 Mass Detector) in positive ion mode and analytical RP-HPLC (Kromasil 300-5-C4 or 300-5-C18 column using a flow rate of 1 mL/min, 5–65% linear gradient of ACN + 0.08% TFA in distilled and deionized water (ddH_2O) + 0.1% TFA over 30 min on a Dionex Ultimate 3000 instrument).

Synthesis of the Scaffold (Y)

The scaffold (**Y**, structure in the Supporting Information) was synthesized on Biotin NovaTag resin (Merck) on a 0.2 mmol scale as described above. Lys(Mtt) was used for selective deprotection and coupling of the PEG_{27} chains, and Boc–Cys(StBu) was used as the N-terminal residue. After the assembly of the peptide chain, the resin was washed with DCM, and then the Mtt groups were selectively removed with DCM/TFA/TIPS (98:1:1, 6×5 min) followed by washing with DCM and then DMF. Monodisperse Fmoc–NH–PEG_{27}–COOH (Polypure, 2.75 equiv) was coupled to the free lysine side chains with 1-[bis-

(dimethylamino)methylene]-1*H*-1,2,3-triazolo[4,5-*b*]-pyridinium 3-oxide hexafluorophosphate (HATU, 2.6 eq, 0.5 M in ACN/DMF 4:6) with DIPEA (5 equiv) overnight. After the removal of the Fmoc protecting groups, Fmoc–propargyl–glycine (5 equiv) was coupled to the PEG chains with HATU (4.8 eq., 0.5 M in DMF) and DIPEA (10 equiv) for 2 h. The N-terminal Fmoc groups were removed, and the peptide was cleaved from the resin and purified as described above.

Synthesis of the Integrin-Targeting Peptide P1

The integrin-binding peptide **P1** (structure in the Supporting Information) was synthesized on Rink Amide MBHA resin on a 0.1 mmol scale with a PEG_3 linker between the Lys(N_3) and the binder peptide sequence. Fmoc–Lys(N_3) was coupled to the resin followed by Fmoc–PEG_3 (16 atoms, Novabiochem) using the standard coupling conditions, and then the **P1** sequence was coupled and the peptide cleaved from the resin and purified as described above.

Synthesis of Y-1

The combined **Y-1** peptide (structure in the Supporting Information) was synthesized on Biotin NovaTag resin on a 0.05 mmol scale as described for the peptide–PEG scaffold except that Fmoc–Lys(ivDde) was used for the first two C-terminal residues, and Boc– Cys(Trt) was used at the N-terminus of the scaffold. Following coupling of the Boc– Cys(Trt), the ivDde protecting groups were removed with 2% hydrazine monohydrate in DMF (3 × 10 min). Fmoc–PEG_{27} was coupled to the lysine side chains as described for the scaffold (**Y**), and then the peptide sequence **P1** was synthesized on both PEG_{27} chains simultaneously, doubling the amount of reagents.

Synthesis of the Scaffold for Cy5-Labeled Y-1

The scaffold for Cy5-labeled **Y-1** (structure in Supporting Information) was synthesized on Rink amide resin on a 0.1 mmol scale with Fmoc–Cys(StBu) as the C-terminal residue. Following assembly of the peptide chain, the N-terminal methionine was formylated with *p*-nitrophenylformate (3 equiv in DMF, 3 h). The Mtt protecting groups were removed from the lysine side chains, and PEG_{27} and propargylglyine were coupled as described for the scaffold **Y**.

Synthesis of Cis- and Oxaliplatin-Based Maleimides and Succinimides

The cis- and oxaliplatin-based platinum(IV) maleimides (*OC*-6-44)-acetatodiamminedichlorido[2-(2,5-dioxo-2,5-dihydro-1*H*-pyrrol-1-yl)ethylcarbamato]-platinum(IV) (**cis-Pt**), and (*OC*-6-34)-acetato[(1*R*,2*R*)-cyclohexane-1,2-diamine]oxalato[2-(2,5-dioxo-2,5-dihydro-1*H*-pyrrol-1-yl)ethylcarbamato]platinum(IV) (**oxali-Pt**) (for ligation to the scaffold **Y**) and succinimide (*OC*-6–34)-acetato-[(1*R*,2*R*)-cyclohexane-1,2-diamine]oxalato[2-(2,5-dioxopyrrolidin-1-yl)ethyl)carbamato]platinum(IV) (**oxali-Pt–succ**) (used as control) were synthesized and characterized as described previously.[17]

CuAAC Reaction of P1 and sc-P1 to the Scaffold Y

CuAAC reactions were performed in degassed solvents, and the reaction vessels were flushed with argon. Stock solutions of $CuSO_4$ (200 mM in ddH_2O), TBTA (100 mM in anhydrous DMF), and sodium ascorbate (500 mM in ddH_2O) were prepared fresh for each reaction. The alkyne-bearing scaffold **Y** and azide-bearing **P1** or **sc-P1** were dissolved in anhydrous DMF in a 2 mL Eppendorf tube flushed with argon. The respective volumes of $CuSO_4$ and TBTA were mixed in a separate tube, followed by the addition of the sodium ascorbate. This mixture was then added to the peptide solution to give final reaction concentrations of the following approximations: peptide–alkyne, 3 mM (1 equiv); peptide–azide, 8 mM (2.5 equiv); $CuSO_4$, 17 mM (6 equiv); sodium ascorbate, 30 mM (10 equiv); TBTA, 19 mM (6.5 equiv); and DMF/H_2O, ~4:1 v/v. The reaction mixture was stirred under argon for 15 min, and the reaction progress was monitored by LC-MS. After completion, the reaction mixture was diluted with water, and the product (**Y-1** or **Y-sc1**) was purified by RP-HPLC.

Ligations of Cis- and Oxaliplatin-Based Maleimides and Cy-5 Maleimide to Y-1

Prior to maleimide ligation, the cysteine thiol group on the scaffold part of **Y-1** was deprotected by incubation of the peptide with TCEP (90 mM in degassed H_2O with pH = 6.5) for 20 min in the dark under argon, followed by purification on an analytical RP-HPLC column (C4). For the maleimide ligation, the **cis-** or **oxali-Pt** maleimide or **Cy-5** maleimide (5 equiv, 7 mM) was dissolved in degassed water and added to **Y-1** (1 equiv, 1.5 mM). The reaction mixture was flushed with argon and stirred for 20 min, and then the product was purified on a RP-HPLC column (C4).

Cell Culture and Transfection of SW480 Cells with Integrin β_6

The human colon carcinoma-derived cell line SW480 (ATCC) as well as the human squamous carcinoma-derived cell line A431 were used in this study. SW480 was grown in minimum essential medium (MEM) and A431 in Roswell Park Memorial Institute medium (RPMI 1640) supplemented with 10% FCS. For the establishment of an integrin β_6-overexpressing cell line, SW480 cells were seeded (3×10^5 cells per well) in six-well plates and allowed to recover for 24 h. Transfection of integrin β_6 pcDNA1 neo-expression plasmid45 (no. 13580, addgene) or with a control plasmid was performed using Lipofectamine 2000 reagent (Invitrogen, Carlsbad, CA) according to the manufacturer's instructions. Medium was changed after 5 h, and selection medium containing 1.2 mg/mL G418 (Sigma, St Louis, MO) was added 24 h after transfection to eliminate nontransfected cells. For further selection of highly integrin β_6-expressing cells, 10^6 transfected cells were sorted by fluorescence-activated cell sorting (FACS) for the highest integrin β_6 expression using a commercially available integrin β_6 antibody conjugated to allophycocyanin (APC, R&D Systems Antihuman Integrin β_6-Allophycoycanin, no. FAB4155A). The highest 5% were resuspended in growth medium for further proliferation. Expression of integrin β_6 was confirmed using Western blot and flow cytometry.

Western Blot Analysis of Integrin Expression

To assess the integrin expression levels, total protein lysates of at least 80%-confluent cells cultivated under normal cell culture conditions were prepared and resolved by sodium dodecyl sulfate polyacrylamide gel electrophoresis (SDS-PAGE) and transferred onto a polyvinylidene difluoride membrane for Western blotting as previously described.[46] The following antibodies were used: integrin β_6 (polyclonal rabbit, dilution of 1:1000) from Santa Cruz Biotechnology Inc., integrin α_V (no. 4711, dilution 1:1000) from Cell Signaling Technology, and β-actin (AC-15; no. A1978, dilution 1:1000) from Sigma-Aldrich. Additionally, horseradish-peroxidase-labeled secondary antibodies from Santa Cruz Biotechnology Inc. were used at working dilutions of 1:10000.

Flow Cytometric Detection of Integrin Expression

Briefly, 2×10^6 cells were trypsinized and incubated in blocking buffer (3% BSA and 5% FCS in PBS) for 10 min on ice. Then anti-integrin β_6 antibody conjugated to allophycocyanine (no. FAB4155A from R&D systems) in blocking buffer was added to a fraction of the cell suspension, resulting in 10^5 cells with a 1:10 dilution of the antibody, and incubated for 75 min on ice. After washing, the cells were analyzed by flow cytometry using a FACS Calibur (Becton Dickinson, Palo Alto, CA). The results were evaluated and quantified using Cell Quest Pro software.

Binding of Biotin–Y-1 and Biotin–Y-sc1 to Integrin β_6-Transfected SW480 Cells

Briefly, 2×10^6 cells were trypsinized and incubated in 1 mL of blocking buffer (PBB–150 mM NaCl, 50 mM Tris-HCl pH 7.5, 5 mM $MgCl_2$, 0.5% Igepal CA-630 containing 4 mM $MnCl_2$) for 10 min on ice. Then, **Y-1** and **Y-sc1**, diluted in PBB (containing 3% BSA, 5% FCS, 5 mM KCl, and 10 mM HEPES in 0.9% NaCl with pH = 7.3), were added in indicated concentrations to 50 μL of the cell suspension and incubated for 30 min on ice. After washing with buffer (10 mM HEPES in 0.9% NaCl with pH = 7.3), cells were resuspended in 1:200 FITC–avidin staining reagent (no. 434411, Life Technologies) in PBB and incubated for 15 min on ice. For analysis, cells were washed and resuspended in phosphate-buffered saline (PBS), followed by flow cytometry using a FACS Calibur (Becton Dickinson, Palo Alto, CA). The results were analyzed and quantified using Cell Quest Pro software.

Cytotoxicity of oxali-Pt–Y-1 against Integrin β_6-Transfected SW480 Cells

For long-term drug exposure, 200 SW480 or SW480 ITGB6 cells per well were seeded in 24 well plates and allowed to recover for 24 h. Then, the cells were exposed to oxaliplatin, **oxali-Pt–succ**, or **oxali-Pt–Y-1** (10 μM) for 14 days. After washing with PBS, the cells were fixed with methanol (–20 °C, 20 min) and after another washing step stained with crystal violet (1 h). The washed and dried plates were then measured for fluorescence (with 633 nm excitation and 610/30 nm BP emission filter) with the imager Typhoon Trio (GE Healthcare Life Sciences). The sum of fluorescence intensities per well was measured with ImageJ and, after blank subtraction, normalized to untreated cells.

Fluorescence Microscopy of Cy5–Y-1 and Biotin–Y-1

Cells were seeded either into 8 well microslides (Ibidi) with 3×10^4 cells per well in 150 μL of growth medium for live-cell microscopy or on 8 spot slides (Thermo Scientific) with 8×10^4 cells/mL for fixed-cell experiments and left to recover for 24 h at 37 °C and 5% CO_2. For the experiment, cells were incubated first with serum-free media for 2 h at 37 °C and then, after washing, treated with **Cy5–Y-1** (0.5 μM) for living cells and **biotin–Y-1** or **biotin–Y-sc1** (1 μM) for fixed-cell experiments in 1% BSA in PBS for 10 min at 37 °C. After a short wash with serum-free phenol-free media, cells stained with **Cy5–Y-1** were imaged quickly at the confocal Zeiss LSM 700 Olympus microscope (Carl Zeiss AG, Oberkochen, Germany). Cells incubated with **biotin–Y-1** were, after washing with PBS, fixed with 4% paraformaldehyde for 20 min on ice, and permeabilized with 0.5% Triton X-100 for 15 min on ice. After another washing step, cells were incubated with 1:200 FITC–avidin (no. 434411, Life Technologies) in 20% FCS in PBS for 20 min on ice and washed again. DAPI (1 μg/mL) in PBS was used as a counterstain with Vectashield (H-1000, Vector Laboratories, Inc., Burlingame, CA) for mounting. Fixed and stained cells were then imaged at the confocal Zeiss LSM 700 Olympus microscope (Carl Zeiss AG, Oberkochen, Germany), and the fluorescence intensity of **biotin–Y-1** per cell area was evaluated with ImageJ.

Cell-Accumulation Experiments of oxali-Pt–Y-1 and Measurement by ICP-MS

According to an optimized protocol,[47] SW480 as well as SW480 ITGB6 cells (3×10^5 cells per well) were seeded in 6 well plates and allowed to recover for 24 h. Then, cells were exposed to 50 μM of either **oxali-Pt–Y-1** or **oxali-Pt–succ** for 3 h. Subsequently, the cells were washed three times with 2 mL of PBS, and platinum was extracted by incubating the cells with 500 μL of HNO_3 (69%, TraceSELECT, Fluka, Buchs, Switzerland) for 1 h. From the suspension, 400 μL was diluted 20-fold in ddH_2O. The experiment was performed in triplicate. Cell-free wells exposed to the same compounds (**oxali-Pt–Y-1** or **oxali-Pt–succ**) were used as blanks. Cells from three additional wells were trypsinized and counted to determine the cell number per well. Ultrapure water (18.2 MΩ cm, Milli-Q Advantage, Darmstadt, Germany) was used for all dilutions for ICP-MS measurements. Nitric acid (69%, TraceSELECT, Fluka, Buchs, Switzerland) was used without further purification. Platinum and rhenium standards for ICP-MS measurements were derived from CPI International (Amsterdam, The Netherlands). All other reagents and solvents were obtained from commercial sources and were used without further purification.

An ICP-MS Agilent 7500ce (Agilent Technologies, Waldbronn, Germany) was equipped with a CETAC ASX-520 autosampler and a MicroMist nebulizer with a sample uptake rate of approximately 0.25 mL/min. The Agilent MassHunter software package (Workstation Software, version B.01.01, build 123.11, patch 4, 2012) was used for data processing. The experimental parameters for ICP-MS are given in Table S1. The instrument was tuned on a daily basis to achieve maximum sensitivity. Rhenium served as an internal standard for all measurements.

Supporting Information

Refer to Web version on PubMed Central for supplementary material.

Acknowledgments

References

(1). Chari RV, Miller ML, Widdison WC. Antibody-drug conjugates: An emerging concept in cancer therapy. Angew Chem, Int Ed. 2014; 53:3796–3827.

(2). Casi G, Neri D. Antibody-drug conjugates: Basic concepts, examples and future perspectives. J Controlled Release. 2012; 161:422–428.

(3). Agarwal P, Bertozzi CR. Site-specific antibody–drug conjugates: The nexus of bioorthogonal chemistry, protein engineering, and drug development. Bioconjugate Chem. 2015; 26:176–192.

(4). Gilad Y, Firer M, Gellerman G. Recent innovations in peptide based targeted drug delivery to cancer cells. Biomedicines. 2016; 4:11.

(5). Wang Y, Cheetham AG, Angacian G, Su H, Xie L, Cui H. Peptide-drug conjugates as effective prodrug strategies for targeted delivery. Adv Drug Delivery Rev. 2017; 110–111:112–126.

(6). Komin A, Russell LM, Hristova KA, Searson PC. Peptide-based strategies for enhanced cell uptake, transcellular transport, and circulation: Mechanisms and challenges. Adv Drug Delivery Rev. 2017; 110–111:52.

(7). Panowski S, Bhakta S, Raab H, Polakis P, Junutula JR. Site-specific antibody drug conjugates for cancer therapy. MAbs. 2014; 6:34–45. [PubMed: 24423619]

(8). Merten H, Brandl F, Pluckthun A, Zangemeister-Wittke U. Antibody-drug conjugates for tumor targeting-novel conjugation chemistries and the promise of non-IgG binding proteins. Bioconjugate Chem. 2015; 26:2176–2185.

(9). Rashidian M, Dozier JK, Distefano MD. Enzymatic labeling of proteins: Techniques and approaches. Bioconjugate Chem. 2013; 24:1277–1294.

(10). Hallam TJ, Wold E, Wahl A, Smider VV. Antibody conjugates with unnatural amino acids. Mol Pharmaceutics. 2015; 12:1848–1862.

(11). Schumacher D, Hackenberger CP. More than add-on: Chemoselective reactions for the synthesis of functional peptides and proteins. Curr Opin Chem Biol. 2014; 22:62–69. [PubMed: 25285752]

(12). Bohme D, Beck-Sickinger AG. Drug delivery and release systems for targeted tumor therapy. J Pept Sci. 2015; 21:186–200. [PubMed: 25703117]

(13). Staben LR, Koenig SG, Lehar SM, Vandlen R, Zhang D, Chuh J, Yu S-F, Ng C, Guo J, Liu Y, et al. Targeted drug delivery through the traceless release of tertiary and heteroaryl amines from antibody–drug conjugates. Nat Chem. 2016; 8:1112–1119. [PubMed: 27874860]

(14). Rostovtsev VV, Green LG, Fokin VV, Sharpless KB. A stepwise huisgen cycloaddition process: copper(I)-catalyzed regioselective "ligation" of azides and terminal alkynes. Angew Chem, Int Ed. 2002; 41:2596–2599.

(15). Tornoe CW, Christensen C, Meldal M. Peptidotriazoles on solid phase: [1,2,3]-triazoles by regiospecific copper(i)-catalyzed 1,3-dipolar cycloadditions of terminal alkynes to azides. J Org Chem. 2002; 67:3057–3064. [PubMed: 11975567]

(16). Pichler V, Mayr J, Heffeter P, Domotor O, Enyedy EA, Hermann G, Groza D, Kollensperger G, Galanksi M, Berger W, et al. Maleimide-functionalised platinum(IV) complexes as a synthetic platform for targeted drug delivery. Chem Commun. 2013; 49:2249–2251.

(17). Mayr J, Heffeter P, Groza D, Galvez L, Koellensperger G, Roller A, Alte B, Haider M, Berger W, Kowol CR, et al. An albumin-based tumor-targeted oxaliplatin prodrug with distinctly improved anticancer activity in vivo. Chem Sci. 2017; 8:2241–2250. [PubMed: 28507680]

(18). Hermanson GT. Bioconjugate techniques. 2nd ed.. Academic Press; London: 2008.

(19). Marelli UK, Rechenmacher F, Sobahi TR, Mas-Moruno C, Kessler H. Tumor targeting via integrin ligands. Front Oncol. 2013; 3:222. [PubMed: 24010121]

(20). Bandyopadhyay A, Raghavan S. Defining the role of integrin $\alpha v \beta 6$ in cancer. Curr Drug Targets. 2009; 10:645–652. [PubMed: 19601768]

(21). Oyama T, Sykes KF, Samli KN, Minna JD, Johnston SA, Brown KC. Isolation of lung tumor specific peptides from a random peptide library: Generation of diagnostic and cell-targeting reagents. Cancer Lett. 2003; 202:219–230. [PubMed: 14643452]

(22). Elayadi AN, Samli KN, Prudkin L, Liu YH, Bian A, Xie XJ, Wistuba II, Roth JA, McGuire MJ, Brown KC. A peptide selected by biopanning identifies the integrin alphavbeta6 as a prognostic biomarker for nonsmall cell lung cancer. Cancer Res. 2007; 67:5889–5895. [PubMed: 17575158]

(23). Mas-Moruno C, Rechenmacher F, Kessler H. Cilengitide: The first anti-angiogenic small molecule drug candidate design, synthesis and clinical evaluation. Anti-Cancer Agents Med Chem. 2010; 10:753–768.

(24). Kapp TG, Rechenmacher F, Neubauer S, Maltsev OV, Cavalcanti-Adam EA, Zarka R, Reuning U, Notni J, Wester HJ, Mas-Moruno C, et al. A comprehensive evaluation of the activity and selectivity profile of ligands for RGD-binding integrins. Sci Rep. 2017; 7 39805.

(25). Zhou X, Chang YC, Oyama T, McGuire MJ, Brown KC. Cell-specific delivery of a chemotherapeutic to lung cancer cells. J Am Chem Soc. 2004; 126:15656–15657. [PubMed: 15571383]

(26). Li S, McGuire MJ, Lin M, Liu YH, Oyama T, Sun X, Brown KC. Synthesis and characterization of a high-affinity $\alpha v \beta 6$-specific ligand for in vitro and in vivo applications. Mol Cancer Ther. 2009; 8:1239–1249. [PubMed: 19435868]

(27). Singh AN, McGuire MJ, Li S, Hao G, Kumar A, Sun X, Brown KC. Dimerization of a phage-display selected peptide for imaging of alphavbeta6- integrin: Two approaches to the multivalent effect. Theranostics. 2014; 4:745–760. [PubMed: 24883124]

(28). Wang D, Lippard SJ. Cellular processing of platinum anticancer drugs. Nat Rev Drug Discovery. 2005; 4:307–320. [PubMed: 15789122]

(29). Johnstone TC, Suntharalingam K, Lippard SJ. The next generation of platinum drugs: Targeted Pt(II) agents, nanoparticle delivery, and Pt(IV) prodrugs. Chem Rev. 2016; 116:3436–3486. [PubMed: 26865551]

(30). Butler JS, Sadler PJ. Targeted delivery of platinum-based anticancer complexes. Curr Opin Chem Biol. 2013; 17:175–188. [PubMed: 23395452]

(31). Conibear AC, Farbiarz K, Mayer RL, Matveenko M, Kahlig H, Becker CF. Arginine side-chain modification that occurs during copper-catalysed azide-alkyne click reactions resembles an advanced glycation end product. Org Biomol Chem. 2016; 14:6205–6211. [PubMed: 27282129]

(32). Enyu L, Zhengchuan N, Jiayong W, Benjia L, Qi S, Ruixi Q, Cheng P, Khan AQ, Wei S, Jun N. Integrin beta6 can be translationally regulated by eukaryotic initiation factor 4E: Contributing to colonic tumor malignancy. Tumor Biol. 2015; 36:6541–6550.

(33). Zhang C, Kimura R, Abou-Elkacem L, Levi J, Xu L, Gambhir SS. A cystine knot peptide targeting integrin alphavbeta6 for photoacoustic and fluorescence imaging of tumors in living subjects. J Nucl Med. 2016; 57:1629–1634. [PubMed: 27230926]

(34). Goschl S, Varbanov HP, Theiner S, Jakupec MA, Galanski M, Keppler BK. The role of the equatorial ligands for the redox behavior, mode of cellular accumulation and cytotoxicity of platinum(IV) prodrugs. J Inorg Biochem. 2016; 160:264–274. [PubMed: 27055943]

(35). Wexselblatt E, Gibson D. What do we know about the reduction of Pt(IV) pro-drugs? J Inorg Biochem. 2012; 117:220–229. [PubMed: 22877926]

(36). Cox N, Kintzing JR, Smith M, Grant GA, Cochran JR. Integrin-targeting knottin peptide-drug conjugates are potent inhibitors of tumor cell proliferation. Angew, Chem Int Ed. 2016; 55:9894–9897.

(37). Kumar A, Mastren T, Wang B, Hsieh JT, Hao G, Sun X. Design of a small-molecule drug conjugate for prostate cancer targeted theranostics. Bioconjugate Chem. 2016; 27:1681–1689.

(38). Yuan Y, Kwok RT, Tang BZ, Liu B. Targeted theranostic platinum(IV) prodrug with a built-in aggregation-induced emission light-up apoptosis sensor for noninvasive early evaluation of its therapeutic responses in situ. J Am Chem Soc. 2014; 136:2546–2554. [PubMed: 24437551]

(39). Mukhopadhyay S, Barnes CM, Haskel A, Short SM, Barnes KR, Lippard SJ. Conjugated platinum(IV)-peptide complexes for targeting angiogenic tumor vasculature. Bioconjugate Chem. 2008; 19:39–49.

(40). Massaguer A, Gonzalez-Canto A, Escribano E, Barrabes S, Artigas G, Moreno V, Marchan V. Integrin-targeted delivery into cancer cells of a Pt(IV) pro-drug through conjugation to RGD-containing peptides. Dalton Trans. 2015; 44:202–212. [PubMed: 25369773]

(41). Gandioso A, Shaili E, Massaguer A, Artigas G, Gonzalez-Canto A, Woods JA, Sadler PJ, Marchan V. An integrin-targeted photoactivatable Pt(IV) complex as a selective anticancer pro-drug: Synthesis and photoactivation studies. Chem Commun. 2015; 51:9169–9172.

(42). Barragan F, Lopez-Senin P, Salassa L, Betanzos-Lara S, Habtemariam A, Moreno V, Sadler PJ, Marchan V. Photocontrolled DNA binding of a receptor-targeted organometallic ruthenium(ii) complex. J Am Chem Soc. 2011; 133:14098–14108. [PubMed: 21797210]

(43). Chin CF, Yap SQ, Li J, Pastorin G, Ang WH. Ratiometric delivery of cisplatin and doxorubicin using tumour-targeting carbon-nanotubes entrapping platinum(iv) prodrugs. Chem Sci. 2014; 5:2265–2270.

(44). Graf N, Bielenberg DR, Kolishetti N, Muus C, Banyard J, Farokhzad OC, Lippard SJ. Alpha(v)beta(3) integrin-targeted plga-peg nanoparticles for enhanced anti-tumor efficacy of a Pt(IV) prodrug. ACS Nano. 2012; 6:4530–4539. [PubMed: 22584163]

(45). Weinacker A, Chen A, Agrez M, Cone RI, Nishimura S, Wayner E, Pytela R, Sheppard D. Role of the integrin alpha v beta 6 in cell attachment to fibronectin. Heterologous expression of intact and secreted forms of the receptor. J Biol Chem. 1994; 269:6940–6948. [PubMed: 8120056]

(46). Heffeter P, Jakupec MA, Korner W, Chiba P, Pirker C, Dornetshuber R, Elbling L, Sutterluty H, Micksche M, Keppler BK, et al. Multidrug-resistant cancer cells are preferential targets of the new antineoplastic lanthanum compound KP772 (FFC24). Biochem Pharmacol. 2007; 73:1873–1886. [PubMed: 17445775]

(47). Egger AE, Rappel C, Jakupec MA, Hartinger CG, Heffeter P, Keppler BK. Development of an experimental protocol for uptake studies of metal compounds in adherent tumor cells. J Anal At Spectrom. 2009; 24:51–61. [PubMed: 22723721]
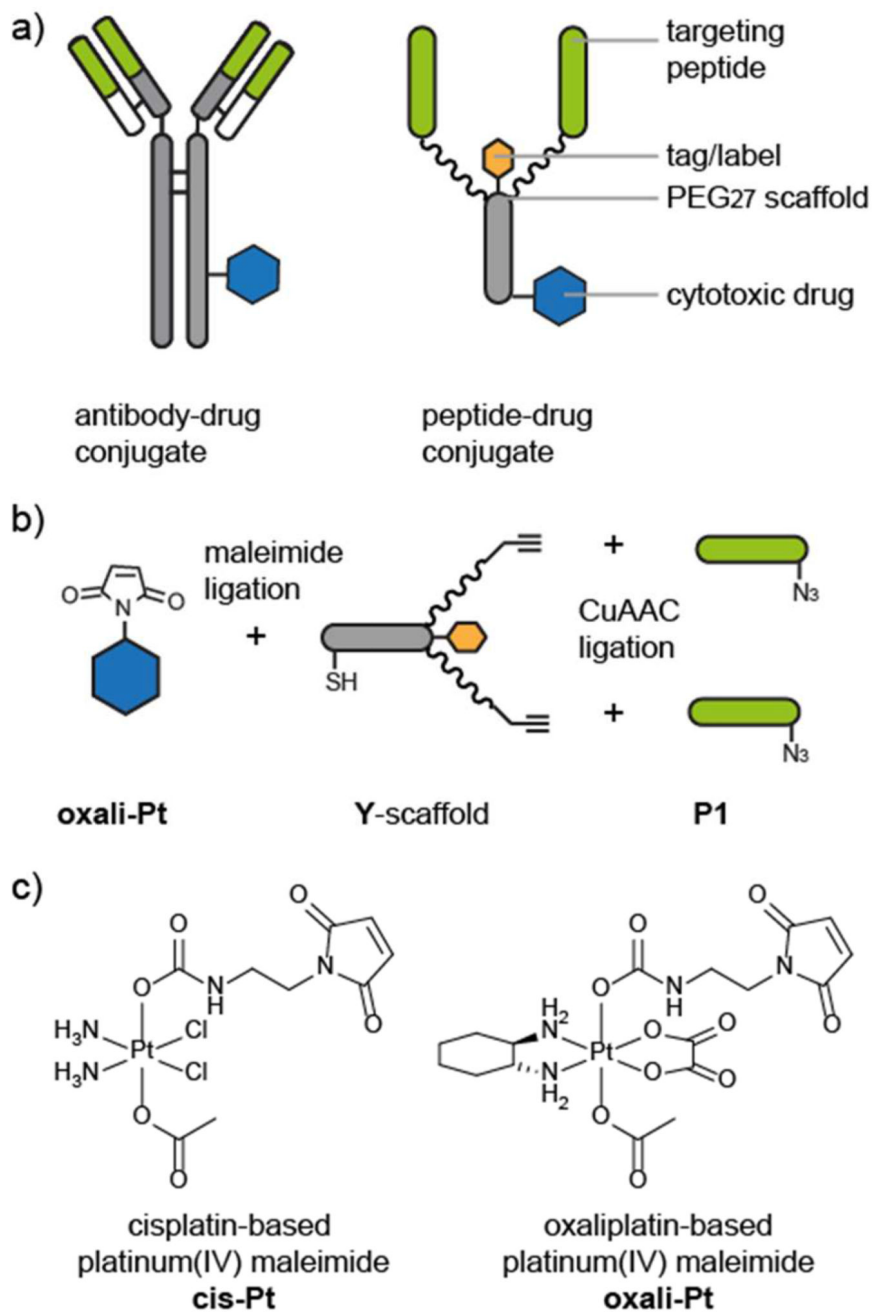
Figure 1. Design and assembly of peptide–drug conjugates.
(a) Comparison between a schematic antibody–drug conjugate and a schematic peptide
–drug conjugate. The antigen-binding regions (green bar) of the antibody bind to specific
receptors on cancer cells and are used to target the cytotoxic drug (blue hexagon) to the
cancer cells. The peptide–drug conjugate is composed of targeting peptides (green) that bind
to cancer cell receptors and a polyethylene glycol (PEG)–peptide scaffold that is conjugated
to the cytotoxic drug. Chemical synthesis allows the inclusion of a label or tag (orange
hexagon) and precise control over the targeting-moiety-to-drug ratio and location. (b)

Modular synthesis and conjugation of the peptide–drug conjugate components. The maleimide-functionalized cytotoxic drug (**oxali-Pt**) is conjugated to a thiol on the peptide –PEG scaffold (**Y**-scaffold). The targeting peptides (**P1**) are conjugated to the scaffold via a copper-catalyzed azide–alkyne click (CuAAC) ligation. (c) Structures of maleimide-functionalized cis- and oxaliplatin-based platinum(IV) complexes **cis-Pt** and **oxali-Pt.**[17]
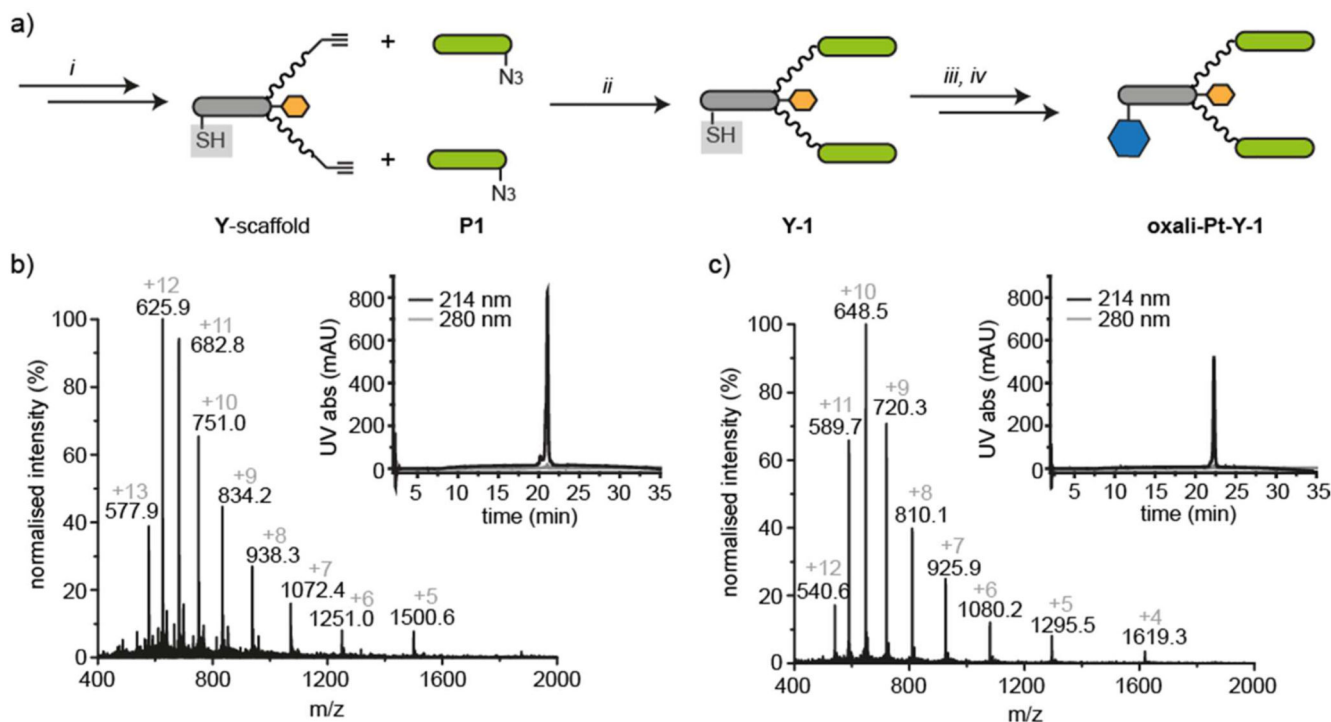
Figure 2. Synthesis and characterization of peptide–drug conjugates.
(a) Solid-phase peptide synthesis (SPPS, i) was used to synthesize the azide-bearing targeting peptides (**P1**, green bar) and the alkyne-bearing peptide–PEG scaffold (**Y**) with the cysteine thiol protected (gray box). CuAAC ligation (ii) was used to conjugate the targeting peptides to the scaffold. The cysteine thiol was then deprotected (iii) and the maleimide-functionalized cytotoxic drug (**oxali-Pt**, blue hexagon) conjugated (iv). (b) ESI-MS and RP-HPLC traces of peptide–drug conjugate (**oxali-Pt–Y-1**) synthesized by modular synthesis (MW_{calc} 7499.5 and MW_{obs} 7499.0). (c) ESI-MS and RP-HPLC traces of peptide–drug conjugate (**oxali-Pt–Y-1**) generated by synthesis of the combined **Y-1** scaffold followed by maleimide ligation of **oxali-Pt** (MW_{calc} 6472.5 and MW_{obs} 6471.3).
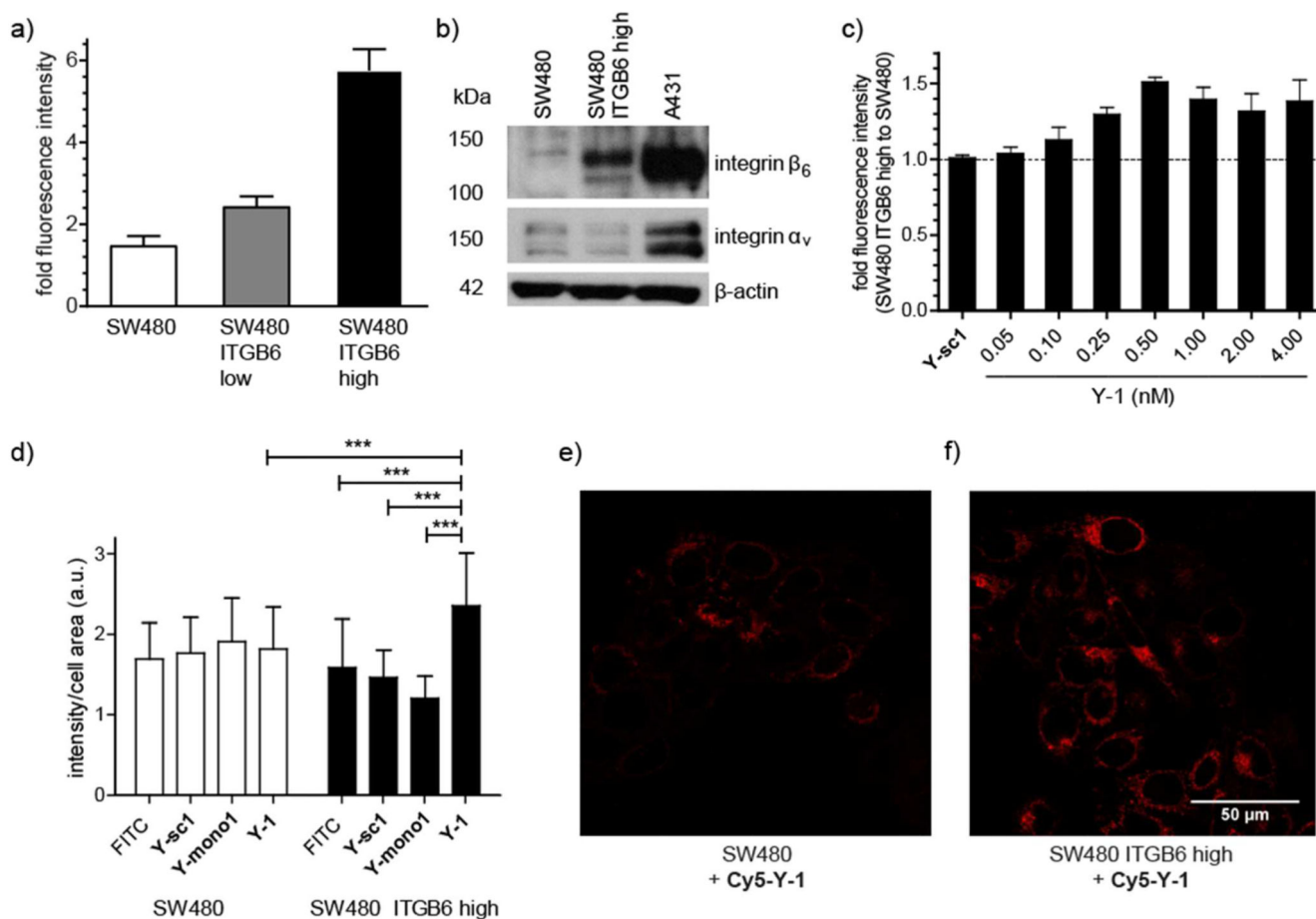
Figure 3. Integrin β_6 transfection of SW480 colon carcinoma cells affects on the binding and uptake of targeted peptides.

(a) Integrin β_6 expression of SW480 cells and transfected cells SW480 ITGB6 low (before sorting) and SW480 ITGB6 high (after sorting) given as fold fluorescence intensity relative to autofluorescence after binding of an antihuman integrin β_6-allophycocyanin antibody and measured by flow cytometry in at least three independent experiments. (b) Integrin β_6 and α_v expression of SW480, SW480 ITGB6 high, and endogenously ITGB6-expressing A431 cells measured of total protein lysates by Western blot. β-actin levels were used as a loading control. Integrin β_6 (MW 97 kDa) and integrin α_v (MW 135−140 kDa). Full gels in Figure S2. (c) Binding of biotinylated **Y-1** and nontargeting scrambled version biotinylated **Y-sc1** (4 nM) to SW480 ITBG6 high compared to non-expressing SW480 cells. Fluorescence of peptide-binding avidin−FITC was measured by flow cytometry and normalized to samples without biotin-labeled peptide. Data is shown as the ratio between SW480 ITGB6 high compared to non-expressing SW480 cells, measured in three independent experiments. (d) Quantification of fluorescence intensity per cell area of confocal microscopy images of SW480 and SW480 ITGB6 high cells incubated with no peptide, 1 μM biotinylated **Y-1**, 1 μM biotinylated **Y-mono-1**, or 1 μM biotinylated **Y-sc1**. Before imaging, cells were fixed, permeabilized, and stained using avidin−FITC (1:200). At least 30 cells of each condition were quantified using ImageJ. (e, f) Confocal microscopy images representing (e) living

SW480 and (f) SW480 ITGB6 high cells exposed to 0.5 μM **Cy5–Y-1** for 10 min at 37 °C (scale bar: 50 μm). Values given in panels a, c, and d are the mean ± standard deviation. Significance was established using one-way ANOVA with Bonferroni's multiple comparison test (***, p 0.001; **, p 0.01; and *, p 0.05).
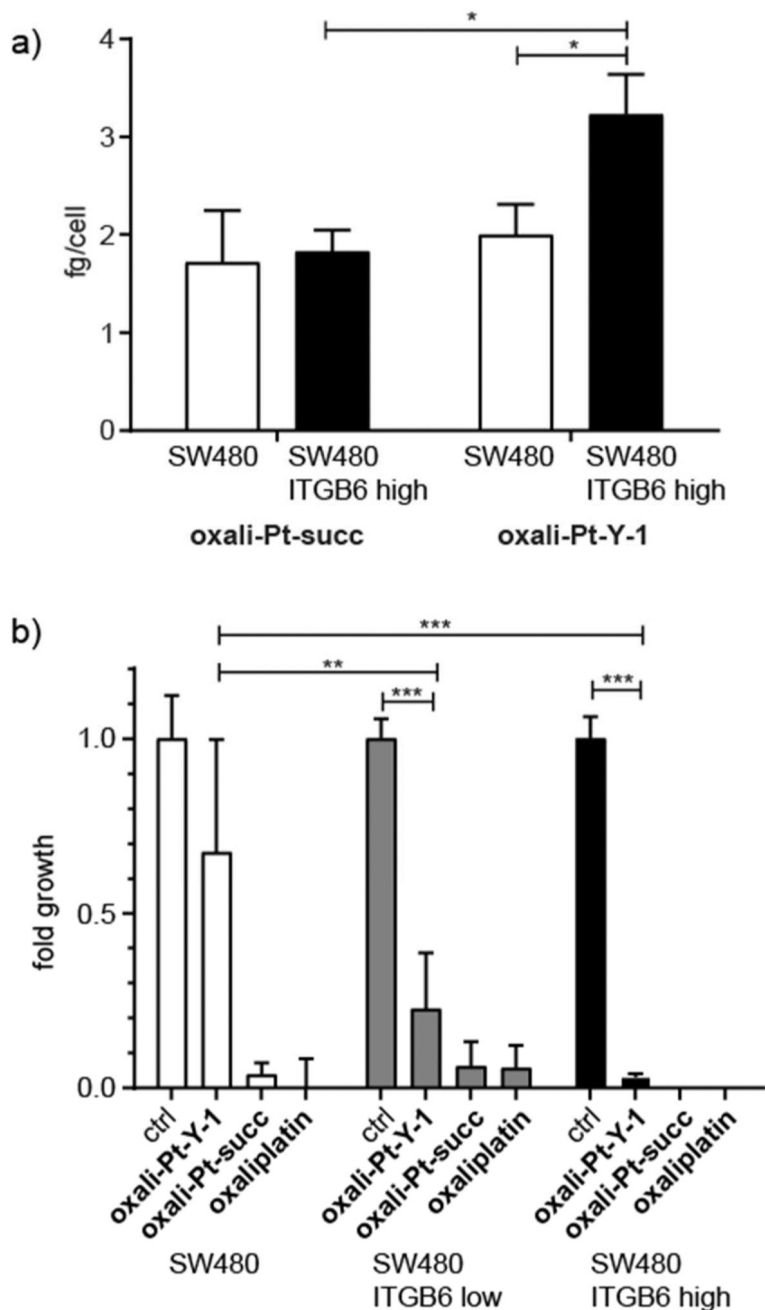
Figure 4. Cellular uptake and cytotoxicity of peptide–drug conjugates in the SW480 model.
(a) Cellular uptake of **oxali-Pt–Y-1** or **oxali-Pt–succ** by SW480 and SW480 ITGB6 high cells. Cells were incubated with 50 μM of either drug for 3 h before isolation and measurement by ICP-MS. The experiment was performed in triplicate. (b) Cytotoxicity of 10 μM **oxali-Pt–Y-1**, **oxali-Pt–succ**, and oxaliplatin after long-term exposure (14 days) to SW480, SW480 ITGB6 low, and SW480 ITGB6 high cells. Cell viability was measured by crystal violet staining from duplicates of three independent experiments. Values given in panels a and b are the mean ± standard deviation, and significances were established using

one-way ANOVA with Bonferroni's multiple comparison test (***, p 0.001; **, p 0.01, and *, p 0.05).